Thermodynamic analysis of the isothermal fractionation of palm oil using a novel method for entrainment correction

Thermodynamic Analysis of the Isothermal Fractionation of Palm Oil using a Novel Method for Entrainment Correction

Elina Hishamuddin[a], Zoltan K. Nagy[b,c] and Andrew G. F. Stapley[b,*]

[a]Product Development and Advisory Services Division, Malaysian Palm Oil Board, 6 Persiaran Institusi, Bandar Baru Bangi, 43000 Kajang, Selangor, Malaysia

[b]Department of Chemical Engineering, Loughborough University, Loughborough, Leicestershire, LE11 3TU, United Kingdom

[c]School of Chemical Engineering, Purdue University, West Lafayette, IN, United States

*Corresponding author. Andrew G. F. Stapley, Department of Chemical Engineering, Loughborough University, Loughborough, Leicestershire, LE11 3TU, United Kingdom.

Email address: A.G.F.Stapley@lboro.ac.uk

[a]Present address.

ABSTRACT

The crystallisation kinetics of individual triacylglycerols (TAGs) were studied during the isothermal fractionation of palm oil. On filtration, entrainment of liquid olein within the stearin cake was found to significantly affect measured solid stearin compositions. These could be corrected for entrainment using a mass balance based method along with the assumption that triunsaturated TAGs did not crystallise. These calculations indicated high olein entrainment levels of ~57-59% within the stearin cake, with typically only ~10% of the palm oil crystallising. These values were validated using pulsed NMR solid fat content measurements. The corrected stearin compositions revealed that diunsaturated TAGs were also virtually absent in the solid phase. Crystallisation was initially dominated by trisaturated TAGs, and later by the monounsaturated TAGs once the trisaturates had depleted from the liquid. The time-course of individual TAG crystallisation rates correlated well with chemical potential driving forces based on temperature and composition information, assuming ideal behaviour.

KEYWORDS. Triacylglycerol, NMR, filtration, chemical potential, solid-fat-content, crystallization driving force.

Highlights

- Crystallization behaviour of triacylglycerols (TAGs) in palm oil fractionation was studied under isothermal conditions.
- Liquid entrainment in stearin cake greatly influenced true stearin composition.
- A method was proposed to quantify entrainment degree and true stearin composition based on TAG composition.
- Crystallisation of diunsaturated TAGs became dominant once trisaturated TAGs depleted from the liquid phase.
- Crystallisation rates of TAGs correlated with chemical potential driving forces based on temperature and composition.

1. Introduction

Palm oil (PO) is the most produced and consumed vegetable oil in the world (Kushairi et al., 2018; Oil World, 2019). The use of PO can be enhanced by a number of modification processes, the most widely practiced and environmentally-friendly of which is through the fractionation of the constituent triacylglycerols (TAGs). Fractionation improves the functionality and characteristics of oils and fats, extending their utilisation to many edible and non-edible applications which may not have been possible in their original form. Since the late 19th century, fractionation has been widely applied to edible oils and fats for the production of feedstocks for margarine, shortenings, frying oils and salad oils, amongst others (Omar et al., 2015). PO has been established in the last four decades as the world's most extensively industrially fractionated vegetable oil.

The fractionation of PO typically produces two distinct fractions; a liquid olein (OL) with enhanced cold stability and a solid stearin (ST) fraction with improved melting properties (Kellens et al., 2007). This is achieved by controlled cooling and agitation of melted oil or fat to induce crystallisation of the higher melting TAGs followed by separation of the ST crystals from the liquid OL (Deffense, 2000). The basis of fractionation is the ability of different TAGs to selectively crystallise owing to the differences in their underlying melting points. During the crystallisation stage, the fat melt undergoes supercooling to below its melting point and the highest melting TAG components begin to crystallise (Hartel, 2013). Previous studies on PO fractionation have shown that in addition to the type, origin and quality of the feed oil, the quality of the OL fraction depends on the separation temperature and holding time at that temperature, whilst the quality of the ST fraction and the yields of both fractions depend on the crystallisation conditions and type of separation process in use (Timms, 2005; Deffense, 2009).

Until now only a limited number of studies have investigated the effect of different fractionation temperatures on the physicochemical properties of the sub-products derived from the fractionation of palm oil (Deffense, 1985; Hasmadi et al., 2002; Zaliha et al., 2004) and blends of palm oil with other liquid oils, i.e. blends of palm oil and sunflower oil (Mamat et al., 2005). The effects of employing different operating temperatures on other oils and fats such as milk fat (Breitschuh and Windhab, 1998; Vanhoutte et al., 2003), butter oil (Fatouh et al., 2003), palm olein (Calliauw et al. 2007), superolein (Huang et al., 2015) and chicken fat (Arnaud and Collignan, 2008) have been studied. These studies have shown that the fractionation conditions, in particular the operating temperature, play an important role in determining the quality of the resultant fractions and their end usage.

The second stage of the fractionation process is the separation of solid TAG crystals from the liquid OL at the fractionation temperature. However, some of the liquid OL remains trapped within the solid TAG crystal network, and this is known as entrainment. The degree of entrainment depends on the crystal morphology, which in turn is affected by the process conditions during crystallisation and the design of the crystalliser, but entrainment levels also depend on the type of separation technique used after the crystallisation stage (Hamm, 1995; Deffense, 1998). Different types of separation processes have been commercially applied over the last couple of decades, ranging from centrifugation, vacuum rotary drum and belt filtration, decanting, and the membrane filter press. However, the membrane filter press remains the preferred technique for the fractionation of PO as higher OL yields can be achieved and entrainment levels are significantly reduced with the increase in squeezing pressures (Timms, 2007). The separation stage is thus as important as the crystallisation stage, since the end product

quality depends significantly on minimising the entrainment of the liquid phase within the solid fraction.

In one of the earliest studies on the determination of entrainment levels in PO crystallisation, entrainment was described as a result of intra-particle (between individual crystals within agglomerates) and inter-particle (between crystal agglomerates) liquid trapped in the filter cake (Bemer and Smits, 1982). The authors proposed a method for calculating entrainment levels based on measurements of the radio-activity of the liquid and slurry concentrations using a liquid scintillation spectrometer. Their study concluded that about 50% of intra-particle liquid remained within PO agglomerates after cake washing with an organic solvent. Since then, many researchers have further proposed various approaches for determining the entrainment level in the solid fraction by using the composition of the OL fractions obtained from filtration (Hamm, 1986), incorporating the iodine value (IV) of the liquid and solid fractions in the mass balance equation of the ST cake (Timms, 1994), and equating entrainment to the degree of porosity in the filter cake produced (Hamm, 2005). It is also possible to use pulsed NMR to provide a direct measurement of the solid fat content (SFC) of either the ST cake (Arnaud and Collignan, 2008) or the crystallising suspension from which it was taken, from which entrainment levels can be deduced (Vanhoutte et al., 2003; Calliauw et al., 2007). Despite the many improvements implemented in the PO fractionation process over the last three decades, entrainment still remains an issue when pursuing a high purity of the solid phase. These studies have repeatedly shown that the filtration stage cannot be regarded as clean and complete. In this aspect, the composition of the solid cake formed will always incorporate an entrainment element and will not represent the true solid crystal composition.

When investigating and optimising fractionation processes, it is obviously necessary to consider the partitioning of TAGs between the solid and liquid phases during the crystallisation process itself. Thermodynamic theories in solid-liquid separation systems have shown that the transformation of liquid to solid is principally governed by the differences in the chemical potential driving forces of the crystallising components between these two phases. The thermodynamic driving force for crystallisation of a TAG species *i*, $\Delta\mu_i$ is fundamentally defined as the difference in chemical potential of the TAG species between the liquid (μ_i^L) and solid (μ_i^S) phases. This is defined as follows (neglecting minor correction terms involving specific heat capacity) (Himawan et al., 2006):

$$\frac{\Delta\mu_i}{RT} = \frac{\Delta H_{m,i}}{R}\left(\frac{1}{T} - \frac{1}{T_{m,i}}\right) + ln\left(\frac{\gamma_i^L x_i^L}{\gamma_i^S x_i^S}\right) \qquad (1)$$

where $\Delta H_{m,i}$ is the molar enthalpy of melting of the pure TAG component *i* at the pure component melting temperature $T_{m,i}$, and γ_i^L and γ_i^S are the activity coefficients of the TAG component *i* in the liquid and solid phases at the temperature, *T* at which crystallisation is taking place.

In fat systems the driving force for crystallisation is usually more simply expressed in terms of either the supersaturation of a component (Van Putte and Bakker, 1987) or the degree of supercooling, $\Delta T = T_{m,i} - T$ (Marangoni and Wesdorp, 2013). Strictly speaking the supercooling should be based on the actual melting point of the component in the solution/mixture concerned, but more often the pure component melting point is used. A recent study on the crystallisation behaviour of PO from different geographic origins using DSC reported that when a low supercooling was applied, the higher melting TAGs were first to crystallise from the melt as the supercooling of the higher melting TAGs are larger than that of lower melting TAGs (Hubbes et

al., 2018). Whilst this is useful in providing a quick, rough guide to behaviour, it should be pointed out that such an approach ignores the reduction in melting point (and hence driving force) that occurs when a species is dissolved in a liquid or melt. This is taken into account in the fuller expression for driving force (**Eq. 1**) which includes the correction for composition. It is also taken into account with supersaturation, but this requires a solubility curve to be available. While the concept of supercooling has long been established with respect to the crystallisation of oils and fats, very few studies have used the fundamental expression for chemical potential driving force (**Eq. 1**), and its application in a dynamic palm oil crystallisation system is still lacking.

The aims of this study are therefore to investigate the effect of different isothermal temperatures on the crystallisation behaviour of palm oil TAGs during fractionation in a stirred system and to explore how the observed behaviour relates to chemical potential driving forces for crystallisation that will be quantified using **Eq. 1** (assuming ideality). A new method for determining the level of entrainment within the filtered solid phase is proposed and compared with the existing pNMR method based upon SFC measurement. The effects of correcting for entrainment on calculating the true solid composition and the thermodynamic driving forces for crystallisation of PO TAGs are also elucidated.

2. Materials and methods

2.1. Materials

Refined, bleached and deodorised (RBD) PO was obtained from Golden Jomalina Sdn. Bhd. (Selangor, Malaysia) and used as raw material for the fractionation experiments. The oil was melted at 70 °C for 1 hour until it was completely melted prior to fractionation. This sample

preparation procedure was standardised for all fractionation experiments carried out in this study. Acetone and acetonitrile used for the TAG compositional analyses were of HPLC-grade (Fisher Scientific, Loughborough, U.K.).

2.2. Fractionation experiments

Fractionation experiments were carried out in a stirred jacketed glass vessel. PO was crystallised at isothermal temperatures (T_{iso}) of 24, 26, 28, 30 and 32 °C. Further details on the experimental set-up, cooling programme and filtration method are described elsewhere (Hishamuddin et al., 2011). The filtered products were subsequently analysed further for their TAG composition. The concentrations of the first five samples of the ST fractions collected at 32°C are not reported as there were insufficient amounts of samples to allow TAG compositional analysis to be performed.

2.3. Triacylglycerols compositional analysis

The TAG compositions of the PO, OL and ST samples from the fractionation experiments were analysed according to the AOCS Official Method Ce 5c-93 (AOCS, 2011) using a HPLC instrument (Model HP 1100 Series, Hewlett Packard, Waldbronn, Germany) with refractive index detection (Agilent 1100 Series, Waldbronn, Germany). TAGs were separated on two identical Waters Nova-Pak© C_{18} columns connected in series (3.9 mm i.d. x 300 mm length, particle size 4 μm) (Waters Corp., Darmstadt, Germany). Minor adjustments were made to the mobile phase composition and injection volume to improve TAG separation. The mobile phase consisted of a mixture of acetone and acetonitrile at a ratio of 63.5:36.5 vol% with a fixed flowrate of 1 mL/min. The injection volume was 10 μL and the columns were maintained at

25°C. TAG peak identification was made based on the retention time of TAG standards and by comparison with literature (Ghazali et al., 1995; Swe et al., 1995; Sulaiman et al., 1997; Haryati et al., 1998). TAG and minor component concentrations were quantified based on peak area normalisation and expressed as weight percentages (wt%). The concentrations of monoacylglycerols and diacylglycerols were not individually quantified and their total concentration was expressed as 'Others'. Reproducibility was assessed by taking triplicate determinations of selected samples, and these showed standard deviations in the range 0.1-0.3 wt% across all TAGs. With this high reproducibility, it was felt to be sufficient to make single HPLC determinations for each sample only. Throughout this entire paper, the major fatty acid moieties present in PO and their abbreviations are denoted as P for palmitic acid (saturated), S for stearic acid (saturated), O for oleic acid (unsaturated) and L for linoleic acid (unsaturated). It should be noted that the HPLC method cannot distinguish or resolve positional isomers. Compositional data are hence labelled with the isomer that is generally accepted as the most abundant, but it should be understood that the data also include contributions from the other isomers. So, for example, data for POP will also include a contribution from PPO.

2.4. Validation of proposed entrainment correction method by pulsed NMR

For the NMR validation experiments, palm oil was isothermally fractionated at nominal fractionation temperatures of 22 °C and 24 °C in a 10 kg stainless steel jacketed crystalliser equipped with a PC controller (Desmet Ballestra, Zaventem, Belgium). In practice, this was achieved on this different system by setting the jacket temperature to 23°C and 25°C respectively which resulted in steady state oil temperatures of 22.4°C and 24.3°C. Samples were taken 260 minutes after crystals were first observed, and analysed as follows:

1. Direct NMR determination of the SFC of the crystallising slurry (no prior filtration).

2. Direct NMR determination of the SFC of the STcake following vacuum filtration.

3. HPLC analysis of the ST cake following vacuum filtration.

4. HPLC of the OL filtrate following vacuum filtration.

5. Relative masses of the ST cake (including entrained OL) and the OL filtrate.

NMR SFC analysis was performed using the direct method by the use of a low-field pulsed NMR (Bruker Minispec mq20, Bruker, Germany) calibrated with three supplied standards (0%, 31.1%, 74.02%). SFC determinations were performed in triplicate.

3. Results and discussion

3.1. TAG compositions of palm oil fractions

The TAG compositions of the final OL and ST fractions obtained from PO crystallisation at all T_{iso} are shown in Table 1. Only the trisaturated (S_3) TAGs are substantially enriched in the ST fraction, with a greater effect at higher T_{iso}. This is expected as the saturated TAG species are more likely to crystallise due to their higher pure component melting temperatures. The disaturated-monounsaturated (S_2U) TAG levels are slightly reduced in the ST, with the other more highly unsaturated TAGs more reduced, showing a lower tendency to crystallise due to their lower pure component melting points and thus lower supercooling of these TAGs at the higher temperatures (Breitschuh and Windhab, 1998). The reductions are less at lower values of T_{iso} which allow more TAGs to be supercooled, increasing the crystallisation of the more unsaturated TAG species (Hubbes et al., 2018).

The S_3 TAGs also show a dramatic decrease in the OL. The compositions of the S_2U, diunsaturated-monosaturated (SU_2) and polyunsaturated (U_3) TAGs in the OL fraction show very

little change for any T_{iso}. The levels of S_2U TAGs appear to be similar to that in the original PO while the SU_2 and U_3 TAGs are slightly higher in the OL, which is in agreement with values reported by previous studies (Deffense, 1985; Kellens et al., 2007). Because of their lower melting points compared to S_3 and S_2U TAGs, SU_2 and U_3 TAG groups remain in a liquid state and are mostly retained in the OL fraction at the temperature range employed in this study. However, a comparable observation with past literature is the presence of an appreciable amount of the SU_2 TAGs, mainly POO and PLO, present in the ST fractions at all temperatures. The presence of SU_2 and U_3 TAGs in the ST is likely due to the entrainment of liquid OL within and between the crystals in the ST cake (Timms, 2005).

3.2. Entrainment Correction Method

Previous research has shown that the occurrence of entrainment during filtration in PO fractionation is the main cause of the considerable amounts of SU_2 and U_3 TAGs still present in the ST (Kellens et al., 2007). Assuming that the majority of SU_2 and U_3 TAGs within PO crystallise in the β' polymorph at the conditions of the experiments, the pure component melting temperatures of these TAGs all lie below 20 °C (De Man and De Man, 2001). In theory, this implies that TAGs containing at least two unsaturated fatty acid components in their structure will not crystallise to any significant extent and only the S_3 and S_2U TAGs should crystallise at the temperatures used in this study.

In order to determine how far entrainment contributes to the error in the TAG composition of the ST fractions, a correction method needs to be implemented. One way to evaluate the entrainment of liquid within a filter cake is by subtracting the percentage of the SFC measured by pulsed NMR from the total fat content (100%) (Arnaud and Collignan, 2008).

However, NMR equipment is not always available, and the method is also highly dependent on strict control of sample temperatures to avoid changes in solid fat content during sampling and transportation of the ST sample to the NMR machine. Here, an alternative method for correcting the ST composition for entrainment is proposed based on composition data of the filtered products, in combination with a mass balance. The method assumes that the U_3 TAGs do not crystallise at all due to their respective pure melting points being below 0 °C, and thus making it unlikely (following **Eq. 1**) that these TAGs will crystallise to any significant extent under the conditions of the crystallisation experiments. The presence of U_3 TAGs present in the ST cake is assumed to be entirely due to entrainment of the OL between the crystals in the ST cake.

The component mass balance for the ST cake is given by:

$$M_E x_i + M_C y_i = (M_E + M_C) z_i \qquad (2)$$

where M_E and M_C are the mass (g) of entrained OL and the mass (g) of crystals within the ST cake, respectively; x and y are the compositions (g TAG/g OL and g TAG/g crystals) of the TAG species i in the corresponding OL fraction and crystals, respectively, and z is the composition (g TAG/g ST) of the corresponding TAG species i in the ST cake (entrained OL plus crystals) after filtration (determined by HPLC).

If it is assumed that a TAG component does not crystallise at the conditions of the experiments (i.e. $y = 0$) and that the TAG composition of the entrained OL is equivalent to that of the residual OL fraction, the entrainment level ($E = M_E/[M_E+M_C]$) within the ST cake can be calculated by rearrangement of **Eq. 2** to give:

$$\frac{M_E}{M_E+M_C} = \frac{z_i}{x_i} = E \qquad (3)$$

where the right-hand side is entirely comprised from experimentally determined mass fractions for the non-crystallising TAG in the ST cake (z) and OL (x) samples, respectively. In the case of

palm oil, three U_3 TAGs are identified to have melting points below zero, namely OOO, OOL and OLL having β' form melting temperatures (T_m) of -11.8 °C, -28.3 °C and -30.2 °C, respectively (De Man, 1999). In this work, the mass fractions used in **Eq. 3** were combined values from all three U_3 TAGs, to minimise experimental error.

To avoid confusion to the reader, throughout this work, the term 'ST' shall henceforth refer to the ST cake collected which contains pure crystals with entrained OL, while the term 'corrected ST composition' will refer to the composition of ST after entrainment correction (pure crystals without entrainment of the OL).

Fig. 1 illustrates the changes in entrainment levels in the ST fractions at all T_{iso} as a function of isothermal time, calculated using **Eq. 3**. It was observed that the levels of entrainment at T_{iso} between 24 and 30 °C were initially high during the early stages of the experiments, with values ranging from 70% to 90% of entrained liquid per total mass of filter cake collected. This may be due to the fact that in the early stages of crystallisation, the crystal sizes will still be very small, with a high surface area to volume ratio and thus occluding a considerable amount of liquid within the crystal network structure. Intraparticle occlusion of the liquid phase may also occur within the growing crystal structure as the amount of liquid gradually increases between dendrites. This is likely a consequence of the uncrystallisable TAG components which are unable to diffuse away fast enough from the crystal surface to avoid becoming entrapped within the crystal growth surrounding it (Harrison et al., 2016).

As the isothermal time progresses, there is a gradual reduction in entrainment levels to between 54% and 65% of the total mass of filter cake, and this remains nearly constant towards the end for all T_{iso}. Among the plausible explanations for these findings is that as time proceeds, crystal growth within the oil bulk causes an overall decrease in the surface area to volume ratio

of the crystals, subsequently entrapping less liquid within the solid crystals. Final entrainment levels within the retentate were higher at lower isothermal temperatures. The entrainment values calculated here were found to be in agreement with values previously reported by several authors (Hamm, 1986; Timms, 2005; Kellens et al., 2007).

The entrainment values from **Fig. 1**, along with the measured mass of the ST cake (including entrained OL) and the measured mass of the OL filtrate allows a true ST yield (total mass fraction of solid in sample taken from the crystalliser) to be calculated. The results show that only about 12% of PO crystallised at 24 °C **(Fig. 2)**. This percentage decreased to slightly less than 9% at higher T_{iso}, except at 32 °C where the level of solids was higher at nearly 11.6%. Hence, based on the corrected ST yields in this study, it can be deduced that typically only about 8-12% of PO crystallises, despite forming a thick slurry.

In addition, once a value for entrainment is calculated it is possible to calculate the true crystal compositions via rearrangement of **Eq. 2:**

$$z_i = \frac{M_E}{M_E+M_C} x_i + \frac{M_C}{M_E+M_C} y_i = E x_i + (1-E) y_i \qquad (4)$$

which leads to

$$y_i = \frac{z_i - E x_i}{1-E} \qquad (5)$$

Table 2 tabulates the TAG composition of the ST crystals calculated after entrainment correction. It is clear that S_3 TAGs showed an overall higher conversion into the solid phase compared to S_2U TAGs. More than 50% of S_3 TAGs are present in the crystals at 24 °C and this increases by about 10% as T_{iso} is increased to 32 °C. S_2U TAGs showed a reduction in their concentration as T_{iso} is increased. On the other hand, SU_2 TAGS are only present at very low concentrations (<6%), further suggesting that the majority of TAGs in this group remain

uncrystallised in the OL. For these TAGs the T_{iso} value is higher than their pure component T_m, so are unlikely to crystallise. However, it is important to validate the entrainment correction method for it to be able to be considered as another general method for predicting entrainment.

3.3. Validation of proposed entrainment correction method

To validate the entrainment correction method, further experiments were performed at nominal fractionation temperatures of 22 °C and 24 °C to compare predictions using this method with those measured directly by pNMR. Two pNMR measurements were made, namely the SFC of the crystallising slurry (corresponding to **Fig. 1**) and the liquid content of the ST sample following vacuum filtration (corresponding to **Fig. 2**). HPLC data were also obtained to provide predictions using the proposed entrainment correction method. A summary of the results is shown in **Table 3**.

It can be seen that there is good agreement between the values predicted by the proposed entrainment correction method using HPLC data and those directly determined by pNMR. Differences in the true solid ST yield predicted by HPLC method and those found with NMR were within experimental error. Less than 2% difference in OL entrainment values are seen.

Values for corrected true ST composition were compared using either NMR or HPLC methods. The NMR method is based on a mass balance of filtered products in conjunction with the NMR SFC content of the crystallliser slurry, following the work of Calliauw et al. (2007). The second method uses the entrainment value derived from the HPLC method as previously described (**Eq. 5**). Values calculated from both methods showed comparable values of S_2U and U_3 TAGs, although higher values of S_3 and lower values of SU_2 TAGs were obtained using the proposed method (**Table 4**).

There is also further evidence supporting the proposed entrainment correction method:
(i) The entrainment levels estimated by this method have proven to be similar to those reported earlier by Timms (2005).
(ii) The entrainment curves (**Fig. 1**) show a consistent trend which is physically plausible.
(iii) Although the method forces the concentration values of the U_3 in the ST fraction to zero, it does not force the values of SU_2, S_2U and S_3 TAGs. The very low values of SU_2 TAGs calculated using this method (**Tables 2 and 4**) provide credibility to the view that U_3 levels will be almost zero (as they would be expected to have lower levels than SU_2 TAGs).

The entrainment correction is useful in decoupling the crystallisation from filtration effects in order to study the two processes independently, and provides a convenient way to estimate the level of entrained OL and true crystals yield. It can be used in the absence of SFC data, for example if pNMR is not available as a technique. It also has a practical advantage over the NMR SFC method in that the ST and OL samples do not require their temperature to be accurately maintained post filtration in the way that the NMR ST samples do.

3.4. Crystallisation rates of TAGs based on corrected ST composition

In this work, the crystallisation rates of PO TAGs were observed by monitoring the relative change in the mass of TAG components in the solid crystal phase as the crystallisation process progresses with time. With a consistent basis of a fixed mass of PO (solid + liquid), the crystallisation yields based on the amount of each TAG in each phase can be determined by multiplying the HPLC mass fraction data by the overall filtration yield of the phase as follows:

$$m_i^f = x_i^f \times \frac{M_f}{\sum_{f=1}^{P} M_f} \qquad (6)$$

where m_i^f is the crystallisation yield expressed as the mass fraction of TAG component *i* in the fraction, *f*, x_i^f is the composition of TAG component *i* in fraction *f*, M_f is the mass of fraction *f* collected during filtration and *P* is the total number of fractions. The amount of an individual TAG in the OL or ST is expressed in terms of g TAG in OL or ST per 100 g of crystallising PO. This was quantified for all TAGs at all T_{iso} and plotted against time. This method allows the variation of masses of individual TAGs in the ST to be followed as the crystallisation progresses. The initial concentration of each TAG at the point of nucleation was taken as zero as it can be presumed that the very first crystal begins appearing at the onset of nucleation and the oil bulk was in a fully melted state at all times prior to the nucleation point. Greater emphasis is placed on the major crystallising TAGs, the concentrations of which are known with much greater percentage accuracy. Hence, the crystallisation rates of individual TAGs were only quantified for TAGs having a concentration larger than 3% in the solid phase, namely PPP, PPS, MPP, POP, PLP and POS (see **Table 2**). Data are presented from the two extremes of temperature tested, namely 24 °C and 32 °C.

Fig. 3 illustrates the progress of crystallisation, m_i^{ST} of the S_3 and S_2U TAGs based on the corrected ST composition at 24 °C and 32 °C. It can be seen that all S_3 TAGs generally showed higher conversion into the solid phase compared to S_2U TAGs when the entrainment correction was taken into account. PPP, in particular, showed a higher rate of transformation into the crystals compared to POP at both temperatures. This observation forms the major difference between the original and the corrected data. When the uncorrected ST composition was used in quantifying m_i^{ST}, at 24 °C both POP and POO appear to have higher conversions into the solid phase compared to PPP (results not shown). **Fig. 3** clearly shows that the crystallisation rate of PPP begins to slow down after 190 minutes at 24 °C, which is much earlier than at 32 °C (220

minutes). The higher degree of supercooling when crystallising at 24 °C would cause a faster depletion of S_3 TAGs from the crystallising slurry, and this would be the main reason for the earlier slowdown with crystallisation rate of S_3 TAGs. These results are consistent with the findings of Harrison *et al*. (2016) which showed that a decline in crystal growth rate in palm oil occurs as a consequence of crystallisable components being consumed from the liquid phase surrounding it, and hence causing a reduction in concentration with time.

In order to ascertain whether the initial assumption applied in the proposed entrainment calculation was correct with regards to the U_3 TAG group not crystallising at all at the conditions of the experiments, the conversion of TAGs into the OL phase was calculated using **Eq. 3**. The only revision in this calculation was that the actual OL mass was taken to be the combined total of the mass of OL collected from filtration and the mass of entrained OL. This was determined based on a mass balance of the filter retentate using the entrainment values calculated earlier.

Fig. 4 depicts the content of TAGs in the OL phase at 24 °C and 32 °C, with separate graphs for major (>5%) and minor (<5%) TAGs for clarity. If the assumption that the U_3 TAGs do not crystallise were true, their mass in the OL phase should remain constant throughout the whole crystallisation. Indeed, the levels of OOO, OOL and OLL remain largely unchanged throughout the whole course of the isothermal crystallisation experiment at 24 °C, further supporting the assumption that U_3 TAGs do not crystallise at this T_{iso}. The SU_2 TAG group, which is comprised mainly of POO, PLO, PLL and SOO, also showed constant levels in the OL throughout the experiment (**Fig. 4a, b**). This finding further suggests that the SU_2 TAGs also barely crystallise at 24 °C, which is expected as the pure melting points of these TAGs lie below 24 °C. Only S_3 TAGs are seen to decrease significantly with time until they reach nearly zero, indicating their depletion from the OL and subsequent conversion into the ST phase (**Fig. 4a**). A

decreasing trend is also observed for S_2U TAGs, but at a more gradual and slower rate compared to S_3 TAGs.

At 32 °C, only the S_3 TAGs showed a considerable depletion from the OL (**Fig. 4c**). All other TAGs with concentrations <5% showed no conversion into the solid phase and remained unchanged throughout the whole duration of the experiment. POP showed a slight depletion from the OL (**Fig. 4d**), suggesting that a very small amount of POP crystallises into the solid phase at 32 °C (this was also observed at 24 °C). PLP, POO and PLO showed constant levels through to the end, signifying that they do not crystallise into the solid phase. Whilst the S_3 TAGs showed considerable reduction in their concentrations, these were not to zero. The final concentrations of these TAGs in the OL phase at the end of the experiment were seen to be slightly higher at 32 °C compared to at 24 °C. This is explained by the lower solubility of the S_3 TAGs at the lower temperature. It can be deduced from these results that among the major TAGs that make up PO, only PPP and POP/PPO which mainly represent the S_3 and S_2U TAG groups crystallise in significant amounts at both 24 °C and 32 °C.

3.5. Crystallisation driving forces of TAGs based on corrected ST composition

Oils and fats generally crystallise from the melt and the driving force in this context is usually expressed in terms of supercooling (ΔT), which is the difference between the melting temperature, T_m and the temperature of the system, T. Due to the relative similarity in size and structure of the TAG molecules, it might be assumed that both the liquid and solid phases behave ideally, thus yielding the activity coefficients in both phases, $\gamma_i^L = 1$ and $\gamma_i^S = 1$ (Wesdorp et al., 2005). In some cases the assumption of ideality may possibly be incorrect but this serves as a

handy approximation nonetheless, in the absence of activity coefficient data. This reduces **Eq. 1** to the following expression for calculating the chemical potential driving force of each TAG:

$$\frac{\Delta\mu_i}{RT} = \frac{\Delta H_{m,i}}{R}\left(\frac{1}{T} - \frac{1}{T_{m,i}}\right) + ln\left(\frac{x_i^L}{x_i^S}\right) \quad (7)$$

It has been reported that palm oil tends to crystallise in the β' form below 34°C (Persmark et al., 1976; Van Putte and Bakker, 1987). For this reason, the assumption that only the β' polymorph was formed at the conditions of the experiments was applied. It was previously shown that the only two TAGs which crystallised in significant amounts based on the corrected ST composition were PPP and POP/PPO. Based on this finding, the crystallisation driving forces ($\Delta\mu$) of PPP and POP shall be considered for comparison purposes. Utilising the corrected ST composition in **Table 2** and values for $T_{m,i}$ and $\Delta H_{m,i}$ for the β' polymorph of pure TAGs obtained from literature (Timms, 1978; Wesdorp et al., 2005), the crystallisation driving forces for PPP and POP were quantified at 24 °C and 32 °C and studied over time.

Fig. 5 illustrates the evolution of the $\Delta\mu$ of PPP and POP at 24 °C and 32 °C. The $\Delta\mu$ of PPP decreased significantly with time when PO was crystallised at 24 °C, indicating that PPP depleted almost entirely from the OL. This follows the considerable reduction in the concentration of PPP in the OL as depicted earlier in **Fig. 4b**. As crystallisation progresses, the $\Delta\mu$ of PPP is then succeeded by that of POP mid-experiment. The $\Delta\mu$ of POP also decreased with time albeit at a much slower rate compared to PPP. This crossover behaviour implies that after 156 minutes, the $\Delta\mu$ of PPP becomes lower than that of POP, hence the slowing down of the crystallisation rate of PPP compared to POP.

At 32 °C, the $\Delta\mu$ of PPP was seen to similarly decrease with time, although at a faster rate than that observed at 24 °C (**Fig. 5b**). This can presumably be attributed to the higher crystallisation temperature employed at 32 °C, where only the S_3 TAGs were likely to crystallise.

The same 'crossover' behaviour between the $\Delta\mu$ of PPP and POP seen at 24 °C could be also observed at 32 °C, where the $\Delta\mu$ of PPP drops to below that of POP at around 216 minutes, bearing negative driving force values towards the end of the experiment. This is due to the large difference between the concentrations of PPP in the OL, which decrease to below 1% (**Table 1**), and values of 40-50% in the ST crystals (**Table 2**). POP showed a minor decrease in $\Delta\mu$, indicating that POP still crystallises at 32 °C but slightly delayed compared to that of PPP. These findings indicate that regardless of the T_{iso}, the sequence in which crystallisation occurs begins with S_3 TAGs due to their higher initial chemical potential driving force which is directly related to the higher T_m of this TAG group. Only once the driving forces for the S_3 TAGs drop below that of the S_2U TAGs, will the crystallisation of the S_2U TAGs begin to predominate. These results further support previous research on TAG behaviour during PO fractionation (Deffense, 1985; Kellens et al., 2007) and fit in with a theoretical framework based on thermodynamic driving force considerations.

4. Conclusions

The effect of isothermal temperature on the partitioning behaviour of TAGs during the crystallisation stage of PO fractionation has been investigated. Liquid entrainment within the ST cake was shown to have a significant influence on the TAG composition of the cake, which did not reflect the true crystal composition. A method to quantify the degree of entrainment, and hence estimate true crystal compositions, was proposed. The basis for the entrainment correction where U_3 TAGs do not crystallise to any significant extent at the conditions of the experiments appears to be valid and predictions of the overall SFC of the crystallising slurry (pre-filtration) and SFC content of the ST cake (post-filtration) agrees with direct measurements using pNMR.

The entrainment correction method proposed here can be used where no NMR facilities exist, and also has an advantage over the NMR method in that accurate temperature control of samples is not necessary post-filtration to ensure accurate results.

Crystallisation yields for each species calculated using the corrected compositions confirm that the crystallisation of S_2U TAGs is delayed compared to S_3 TAGs, and only become the dominant crystallising species once the S_3 TAGs have depleted from the melt. This study has demonstrated that the crystallisation rates of PO TAGs are well correlated with a fundamental expression for chemical potential driving forces based upon both temperature and composition (**Eq. 1**). These reflect the real decrease in driving force as components are depleted from the melt. This is in contrast to the more commonly used concept of supercooling , $\Delta T = T_{m,i} - T$ (Marangoni and Wesdorp, 2013) based on pure component melting points which would fail to describe this drop-off in crystallisation rates, as this quantity would remain constant (by definition) during the entire isothermal period.

Acknowledgements

The first author gratefully acknowledges the Malaysian Palm Oil Board for a PhD scholarship. The authors thank staff from the Innovative Products Group at the Malaysian Palm Oil Board for their technical assistance.

References

AOCS (2011). AOCS Official Method Ce 5c-93. Individual triglycerides in oils and fats by HPLC, *Official Methods and Recommended Practices of the American Oil Chemists' Society*, 6th ed., AOCS Press, Champaign.

Arnaud, E., & Collignan, A. (2008). Chicken fat dry fractionation: effects of temperature and time on crystallization, filtration and fraction properties. *European Journal of Lipid Science and Technology*, 110(3), 239-244.

Bemer, G. G., & Smits, G. (1982). Industrial Crystallisation of Edible Fats: Levels of Liquid Occlusion in Crystal Agglomerates. In *Proceedings of the Eight Symposium on Industrial Crystallisation*, Amsterdam, The Netherlands.

Breitschuh, B., & Windhab, E. J. (1998). Parameters influencing cocrystallization and polymorphism in milk fat. *Journal of the American Oil Chemists' Society*, 75(8), 897-904.

Calliauw, G., Gibon, V., De Greyt, W., Plees, L., Foubert, I., & Dewettinck, K. (2007). Phase composition during palm olein fractionation and its effect on soft PMF and superolein quality. *Journal of the American Oil Chemists' Society*, 84(9), 885-891.

Deffense, E. (1985). Fractionation of palm oil. *Journal of the American Oil Chemists' Society*, 62(2), 376-385.

Deffense, E. (1998). Dry fractionation and selectivity: Innovations technologiques. *OCL. Oléagineux, Corps gras, Lipides*, 5(5), 391-395.

Deffense, E. (2000). Dry fractionation technology in 2000. *European Journal of Lipid Science and Technology*, 102(3), 234-236.

Deffense, E. (2009). From organic chemistry to fat and oil chemistry. *Oléagineux, Corps gras, Lipides*, 16(1), 14-24.

De Man, J. M. (1999). Relationship among chemical, physical and textural properties of fats. In N. Widlak, (Ed.), *Physical properties of fats, oils and emulsifiers* (pp. 79-95). AOCS Press, Champaign.

De Man, J. M., & De Man, L. (2001). Polymorphism and Texture of Fats. In N. Widlak, R. Hartel, S. Narine (Eds.), *Crystallization and Solidification Properties of Lipids* (pp. 225-235). AOCS Press, Champaign.

Fatouh, A. E., Singh, R. K., Koehler, P. E., Mahran, G. A., El-Ghandour, M. A., & Metwally, A. E. (2003). Chemical and thermal characteristics of buffalo butter oil fractions obtained by multi-step dry fractionation. *LWT-Food Science and Technology*, 36(5), 483-496.

Ghazali, H. M., Hamidah, S., & Che Man, Y. B. (1995). Enzymatic transesterification of palm olein with nonspecific and 1, 3-specific lipases. *Journal of the American Oil Chemists' Society*, 72(6), 633-639.

Hamm, W. (1986). Fractionation-With or without Solvent?. *Fette, Seifen, Anstrichmittel*, 88(S1), 533-537.

Hamm, W. (1995). Trends in edible oil fractionation. *Trends in Food Science & Technology*, 6(4), 121-126.

Hamm, W. (2005). Entrainment: Are We Making Progress? In *Society of Chemical Industry (SCI) Oils and Fats Group Meeting on Fractionation – Current Status and Future Prospects in a Low-Trans World*, Ghent, Belgium.

Harrison, P. D., Smith, K. W., Bhaggan, K., & Stapley, A. G. F. (2016). Image analysis of palm oil crystallisation as observed by hot stage microscopy. *Journal of Crystal Growth*, 444, 28-38.

Hartel, R. W. (2013). Advances in food crystallization. *Annual Review of Food Science and Technology*, 4, 277-292.

Haryati, T., Man, Y. C., Ghazali, H. M., Asbi, B. A., & Buana, L. (1998). Determination of iodine value of palm oil based on triglyceride composition. *Journal of the American Oil Chemists' Society*, 75(7), 789-792.

Hasmadi, M., Aini, I. N., Mamot, S., & Yusof, M. S. A. (2002). The effect of different types of stirrer and fractionation temperatures during fractionation on the yield, characteristics and quality of oleins. *Journal of Food Lipids*, 9(4), 295-307.

Himawan, C., Starov, V. M., & Stapley, A. G. F. (2006). Thermodynamic and kinetic aspects of fat crystallization. *Advances in Colloid and Interface Science*, 122(1-3), 3-33.

Hishamuddin, E., Stapley, A. G. F., & Nagy, Z. K. (2011). Application of laser backscattering for monitoring of palm oil crystallisation from melt. *Journal of Crystal Growth*, 335(1), 172-180.

Huang, X., Wang, J., Ouyang, J., Hao, H., Wang, Y., Gao, Y. Yin, Q., & Bao, Y. (2015). Correlation between thermal properties and chemical composition of palm oil top olein fractions. *Chemical Engineering & Technology*, 38(6), 1035-1041.

Hubbes, S. S., Danzl, W., & Foerst, P. (2018). Crystallization kinetics of palm oil of different geographic origins and blends thereof by the application of the Avrami model. *LWT*, 93, 189-196.

Kellens, M., Gibon, V., Hendrix, M., & De Greyt, W. (2007). Palm oil fractionation. *European Journal of Lipid Science and Technology*, 109(4), 336-349.

Kushairi, A., Loh, S. K., Azman, I., Hishamuddin, E., Ong-Abdullah, M., Izuddin, Z. B. M. N., Razmah, G., Sundram, S., & Parveez, G. K. A. (2018). Oil palm economic performance in Malaysia and R&D progress in 2017. *Journal of Oil Palm Research*, 30(2), 163-195.

Mamat, H., Aini, I. N., Said, M., & Jamaludin, R. (2005). Physicochemical characteristics of palm oil and sunflower oil blends fractionated at different temperatures. *Food Chemistry*, 91(4), 731-736.

Marangoni, A. G.; Wesdorp, L. H. (2013). Nucleation and Crystalline Growth Kinetics. In A. G. Marangoni, L. H. Wesdorp (Eds.), *Structure and properties of fat crystal networks* (pp. 27-100). CRC Press, Boca Raton.

Oil World ISTA Mielke GmbH (2019). *OIL WORLD Statistics Update*, June 2019.

Omar, Z., Hishamuddin, E., Sahri, M.M., Fauzi, S.H.M., Dian, N.L.H.M., Ramli, M.R., Abd. Rashid, N. (2015). Palm oil crystallization: A review. *Journal of Oil Palm Research*, 27(2), 97-106.

Persmark, U., Melin, K. A., & Stahl, P. O. (1976). Palm oil, its polymorphism and solidification properties. *Rivista Italiana delle Sostanze Grasse (Italy)*, LIII, 301-306.

Swe, P. Z., Man, Y. C., & Ghazali, H. M. (1996). Improved NARP-HPLC method for separating triglycerides of palm olein and its solid fractions obtained at low temperature storage. *Food Chemistry*, 56(2), 181-186.

Sulaiman, M. Z., Sulaiman, N. M., & Kanagaratnam, S. (1997). Triacylglycerols responsible for the onset of nucleation during clouding of palm olein. *Journal of the American Oil Chemists' Society*, 74(12), 1553-1558.

Timms, R. E. (1978). Heats of fusion of glycerides. *Chemistry and Physics of Lipids*, 21(1-2), 113-129.

Timms, R. E. (1994). Principles of Fat Fractionation. In *SCI Lecture Paper Series, Society of Chemical Industry (SCI) Oils and Fats Group Symposium on Fractional Crystallisation of Fats*, London, UK.

Timms, R. E. (2005). Fractional crystallisation–the fat modification process for the 21st century. *European Journal of Lipid Science and Technology*, 107(1), 48-57.

Timms, R. E. (2007). Fractionation of palm oil: Current status, future possibilities. *Inform*, 18, 59-62.

Vanhoutte, B., Dewettinck, K., Vanlerberghe, B., & Huyghebaert, A. (2003). Monitoring milk fat fractionation: filtration properties and crystallization kinetics. *Journal of the American Oil Chemists' Society*, 80(3), 213-218.

Van Putte, K. P. A. M., & Bakker, B. H. (1987). Crystallization kinetics of palm oil. *Journal of the American Oil Chemists' Society*, 64(8), 1138-1143.

Wesdorp, L. H., Van Meeteren, J. A., De Jong, S., Giessen, R. V. D., Overbosch, P., Grootscholten, P. A. M., Struik, M., Royers, E., Don, A., De Loos, T., Peters, C., & Gandasasmita, I. (2005). Liquid-Multiple Solid Phase Equilibria in Fats: Theory and Experiments. In A. J. Marangoni (Ed.), *Fat Crystal Networks* (pp. 481 – 711). Marcel Dekker, New York.

Zaliha, O., Chong, C. L., Cheow, C. S., Norizzah, A. R., & Kellens, M. J. (2004). Crystallization properties of palm oil by dry fractionation. *Food Chemistry*, 86(2), 245-250.

Table 1. TAG composition of PO feed, the final OL and ST fractionated at different isothermal temperatures (T_{iso})

TAG (%)	PO	OL (final samples)					ST (final samples)				
		24 °C	26 °C	28 °C	30 °C	32 °C	24 °C	26 °C	28 °C	30 °C	32 °C
PPP	4.8	0.4	0.7	1.3	1.0	0.8	14.4	16.8	20.9	22.6	23.6
POP	28.0	27.4	28.0	27.8	27.7	28.5	29.3	28.0	27.7	27.3	26.7
POO	24.0	26.6	25.8	25.4	25.5	25.3	18.2	18.3	16.3	15.1	15.3
OOO	4.2	4.8	4.7	5.1	4.6	5.0	3.0	3.0	2.6	2.9	2.6
PPS	0.9	ND	ND	0.1	0.1	0.2	2.6	3.0	3.8	4.2	3.7
MPP	0.5	0.1	0.4	0.2	0.2	0.5	1.2	1.7	1.5	1.5	1.7
PLP	9.1	9.8	9.5	9.4	9.3	9.3	8.1	7.7	7.6	7.5	7.7
POS	4.5	4.5	4.5	4.5	5.1	4.7	4.6	4.1	4.5	3.9	3.7
MLP	0.7	0.5	0.8	0.7	0.8	0.9	0.4	0.4	0.6	0.5	0.6
SOS	0.5	0.5	0.8	0.9	0.6	0.3	0.4	1.0	0.3	0.3	0.4
PLO	10.6	11.9	11.6	11.4	11.6	11.6	7.8	7.2	6.3	6.5	6.4
SOO	2.3	2.5	2.5	2.8	2.6	2.4	1.9	1.5	1.3	1.3	1.3
PLL	2.1	2.5	2.4	2.1	2.5	2.2	1.6	1.2	1.2	1.3	1.4
OOL	1.9	2.1	2.0	2.1	2.2	2.0	1.4	1.3	1.3	1.1	1.2
OLL	0.5	0.4	0.5	0.4	0.5	0.5	0.4	0.2	0.3	0.3	0.3
S_3	6.2	0.5	1.1	1.6	1.3	1.5	18.2	21.5	26.2	28.3	29.0
S_2U	42.8	42.7	43.6	43.3	43.5	43.7	42.8	41.2	40.7	39.5	39.1
SU_2	39.0	43.5	42.3	41.7	42.2	41.5	29.5	28.2	25.1	24.2	24.4
U_3	6.6	7.3	7.2	7.6	7.3	7.5	4.8	4.5	4.2	4.3	4.1

Note: TAG concentrations given in wt% of total normalised peak area; ND, not detected; Data include any positional isomers of quoted TAG.

Table 2. Calculated TAG composition of ST crystals after entrainment correction

TAG (%)	Corrected ST composition (final samples) (wt%)				
	24 °C	26 °C	28 °C	30 °C	32 °C
PPP	40.9	44.2	44.1	53.2	49.9
POP	32.9	28.0	27.4	26.7	24.6
POO	2.4	5.6	5.5	0.4	3.7
OOO	-0.4	0.2	-0.3	0.5	-0.2
PPS	7.5	8.2	8.0	9.9	7.8
MPP	3.2	3.8	3.1	3.3	3.1
PLP	5.0	4.5	5.4	4.9	5.7
POS	4.7	3.5	4.4	2.1	2.6
MLP	0.2	-0.4	0.4	0.1	0.3
SOS	0.2	1.2	-0.4	-0.1	0.5
PLO	0.1	-0.3	0.3	-0.7	0.4
SOO	0.3	-0.2	-0.4	-0.6	-0.1
PLL	0.1	-0.6	0.2	-0.4	0.5
OOL	0.1	0.0	0.2	-0.4	0.2
OLL	0.3	-0.2	0.1	-0.1	0.0
S_3	51.6	56.2	55.2	66.4	60.8
S_2U	43.0	36.8	37.2	33.7	33.7
SU_2	2.9	4.5	5.6	-1.3	4.5
U_3	0.0	0.0	0.0	0.0	0.0

Note: Data include any positional isomers of quoted TAG.

Table 3. Comparison of ST yield (wt% solids in crystalliser) and OL entrainment (wt% liquid in filter cake) determined from the proposed entrainment correction method ("HPLC method") and via direct measurement using the NMR SFC method.

Nominal fractionation temperature (°C)	ST Yield (wt%)		OL Entrainment (wt%)	
	HPLC method	NMR SFC method	HPLC method	NMR SFC method
22	12.7±0.2	12.5±0.1	58.1±0.7	59.9±0.3
24	12.3±0.1	12.3±0.3	57.7±0.3	59.0±0.2

Table 4. Comparison of true TAG compositions of ST (final samples) corrected for entrainment using NMR SFC values of the crystalliser slurry (based on Calliauw et al., 2007), and entrainment values derived from HPLC data

TAG	Corrected ST composition (final samples) (wt%)			
	Using NMR SFC data		Using HPLC correction method	
	22 °C	24 °C	22 °C	24 °C
PPP	43.7	43.9	47.4	47.3
POP	28.2	27.4	28.3	26.9
POO	4.4	3.9	1.0	1.3
OOO	0.6	0.0	-0.1	-0.1
PPS	8.3	8.4	8.9	9.1
MPP	3.2	3.1	3.5	3.4
PLP	4.4	4.3	4.0	5.1
POS	3.4	3.9	4.5	4.5
MLP	0.0	0.5	0.1	0.2
SOS	0.6	0.3	0.4	0.2
PLO	0.4	0.7	-0.2	-0.8
SOO	0.5	0.5	0.3	0.5
PLL	-0.1	0.3	-0.1	-0.1
OOL	0.2	-0.2	0.1	0.1
OLL	0.1	0.0	0.0	0.0
S_3	55.2	55.4	59.8	59.8
S_2U	36.6	36.4	37.3	36.9
SU_2	5.2	5.4	1.0	0.9
U_3	0.9	-0.2	0.0	0.0

Note: Data include any positional isomers of quoted TAG.

Figure captions

Fig. 1. Entrainment levels in ST fractions at different T_{iso} as a function of time.

Fig. 2. Corrected ST yield (%) at each T_{iso} calculated from the proposed entrainment correction method as a function of time

Fig. 3. Crystallisation rates of TAGs in crystals per 100g palm oil (based on corrected ST composition) as a function of time at (a) 24 °C and (b) 32 °C

Fig. 4. Crystallisation rates of TAGs in OL (based on corrected ST composition) for (a) TAG <5% at 24 °C, (b) TAG >5% at 24 °C, (c) TAG <5% at 32 °C and (d) TAG >5% at 32 °C.

Fig. 5. Crystallisation driving force versus temperature for PPP and POP (based on corrected ST composition) at (a) 24 °C and (b) 32 °C.

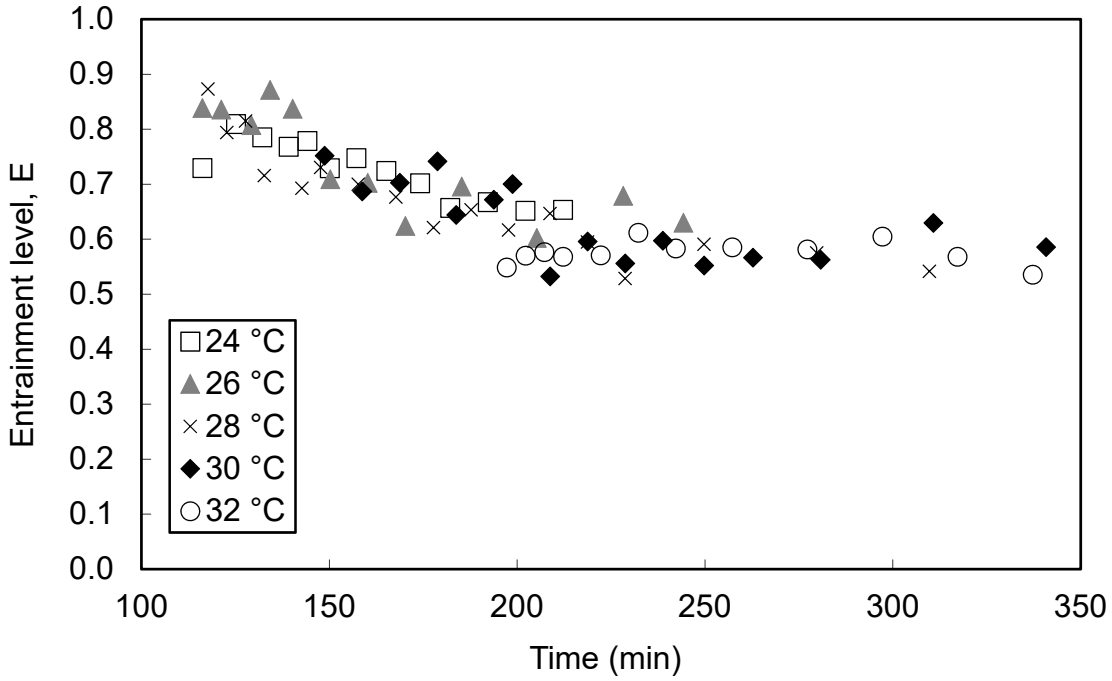
Entrainment level, E
Time (min)
24 °C
26 °C
28 °C
30 °C
32 °C

Fig. 1

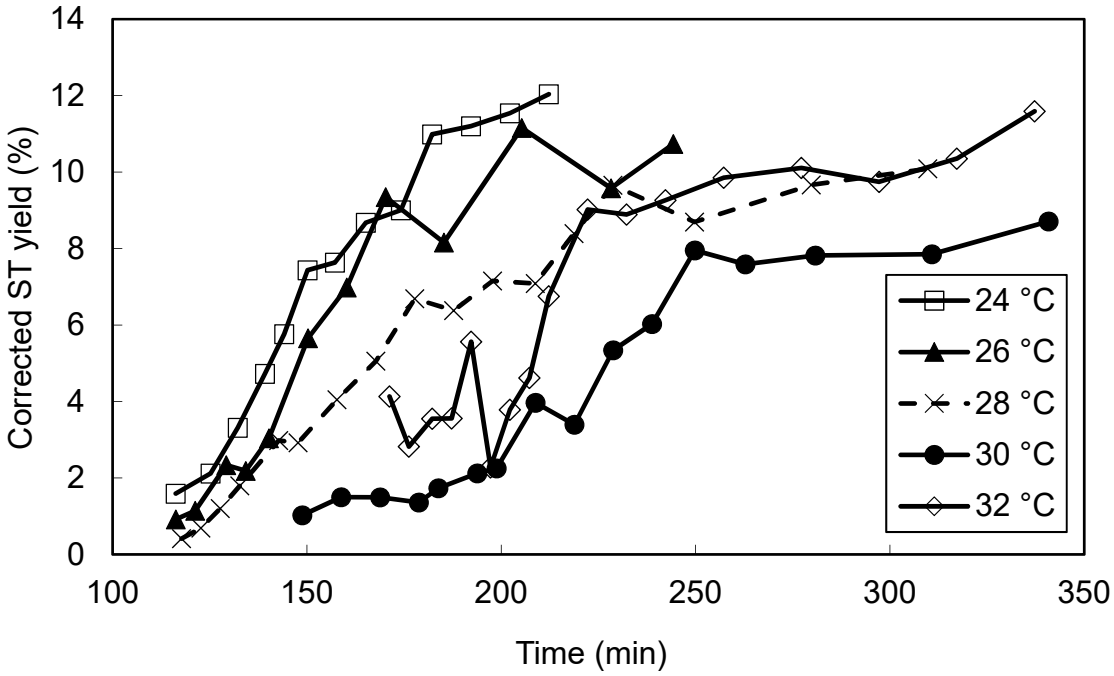
Corrected ST yield (%)
Time (min)
24 °C
26 °C
28 °C
30 °C
32 °C

Fig. 2

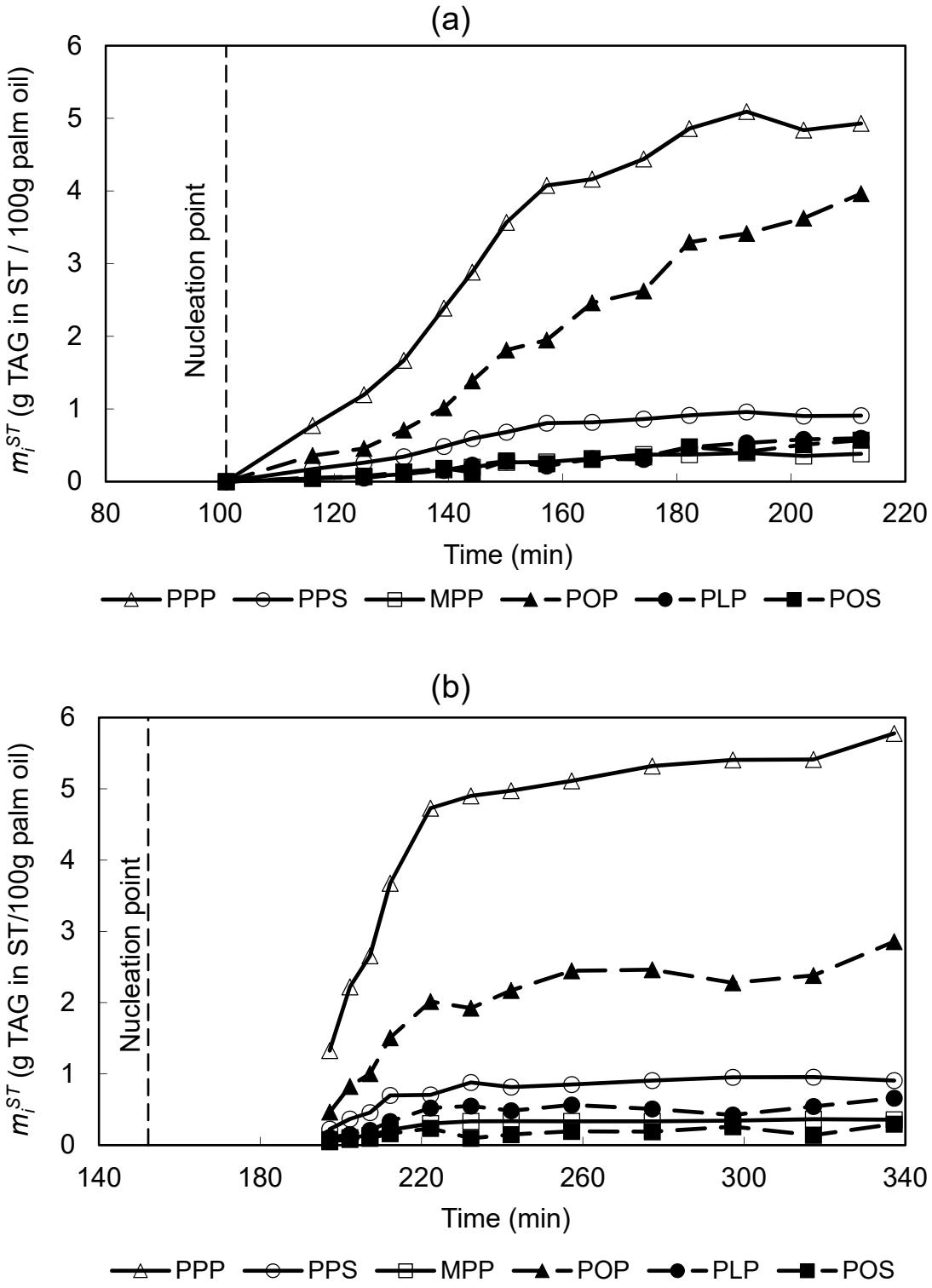
(a)
m_i^{ST} (g TAG in ST / 100g palm oil)
Nucleation point
Time (min)
PPP
PPS
MPP
POP
PLP
POS
(b)
m_i^{ST} (g TAG in ST/100g palm oil)
Nucleation point
Time (min)
PPP
PPS
MPP
POP
PLP
POS

Fig. 3

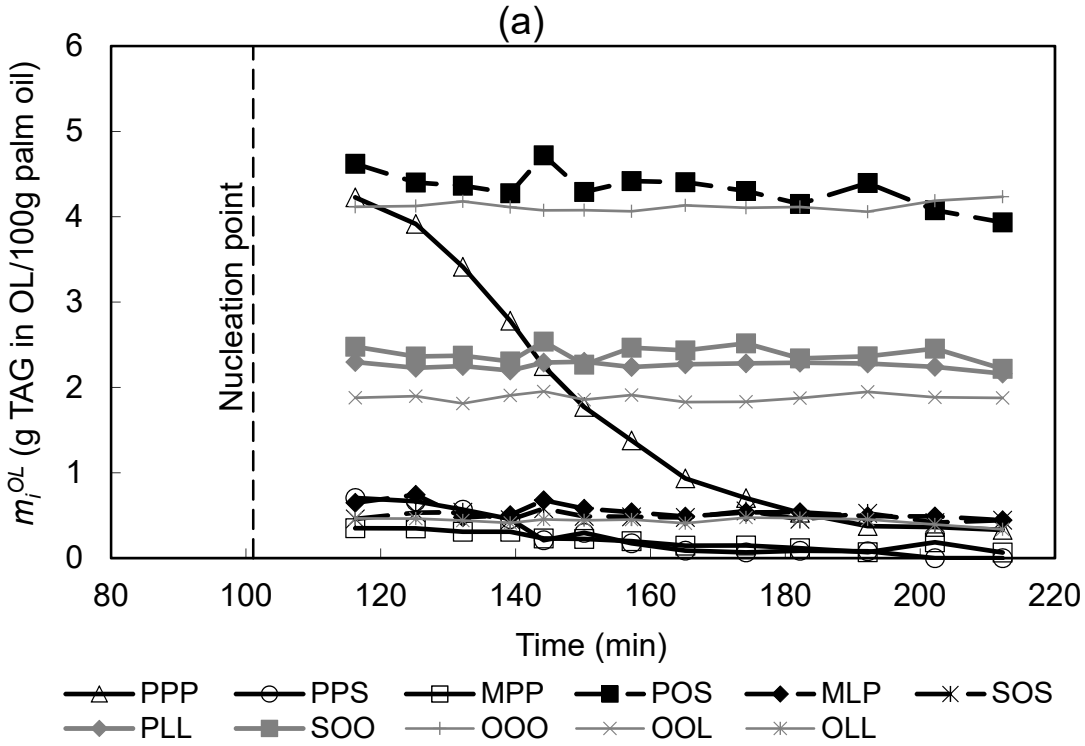
(a)
m_i^{OL} (g TAG in OL/100g palm oil)
Nucleation point
Time (min)
PPP
PPS
MPP
POS
MLP
SOS
PLL
SOO
OOO
OOL
OLL

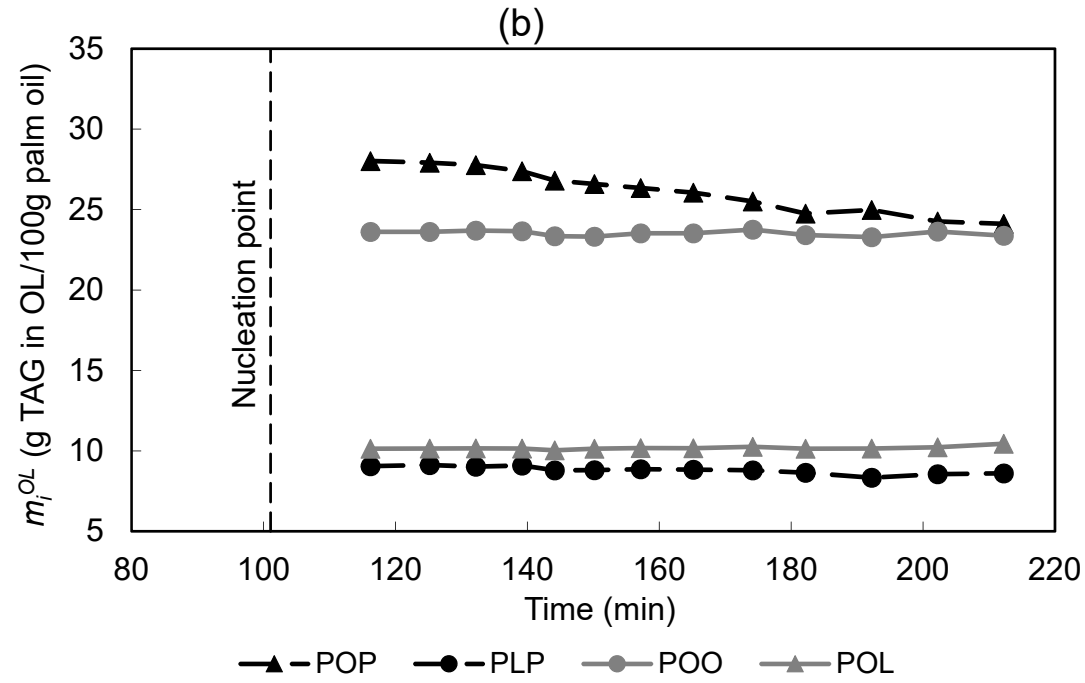
(b)
m_i^{OL} (g TAG in OL/100g palm oil)
Nucleation point
Time (min)
POP
PLP
POO
POL

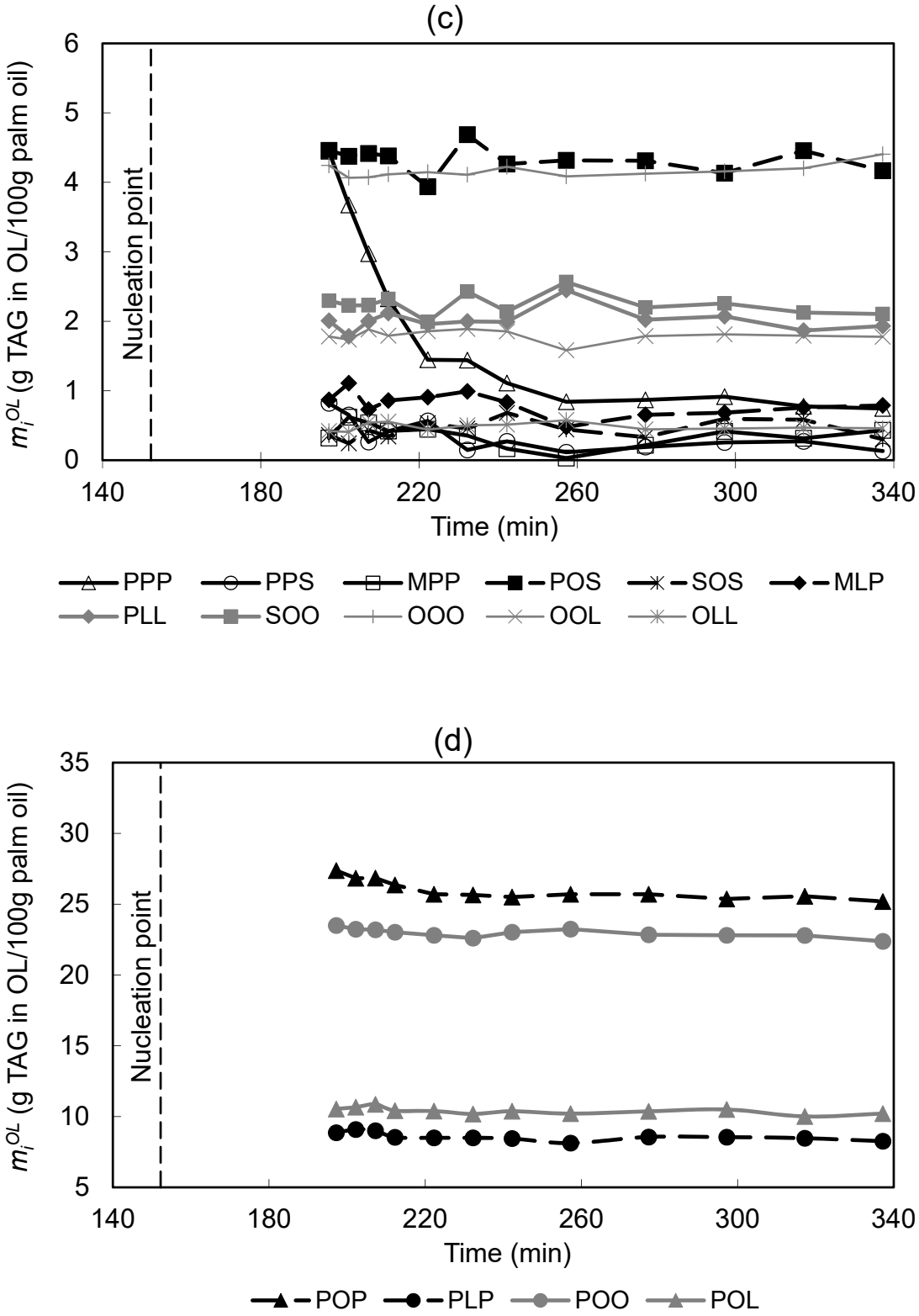
(c)
m_i^{OL} (g TAG in OL/100g palm oil)
Nucleation point
Time (min)
PPP
PPS
MPP
POS
SOS
MLP
PLL
SOO
OOO
OOL
OLL
(d)
m_i^{OL} (g TAG in OL/100g palm oil)
Nucleation point
Time (min)
POP
PLP
POO
POL

Fig. 4

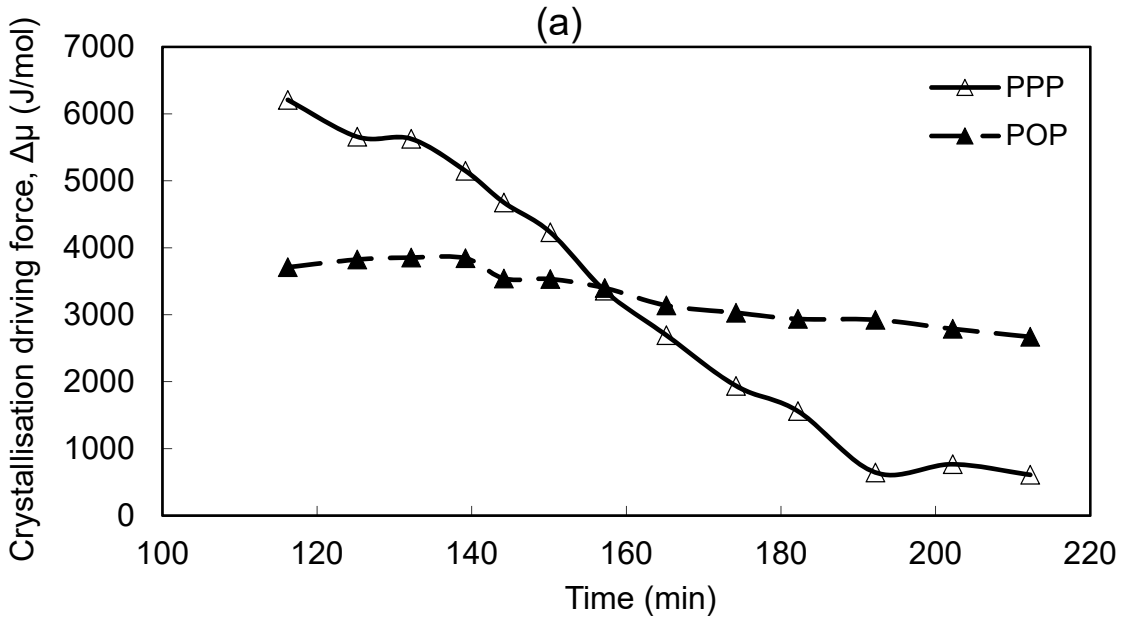
(a)
Crystallisation driving force, Δμ (J/mol)
7000
6000
5000
4000
3000
2000
1000
0
100
120
140
160
180
200
220
Time (min)
PPP
POP

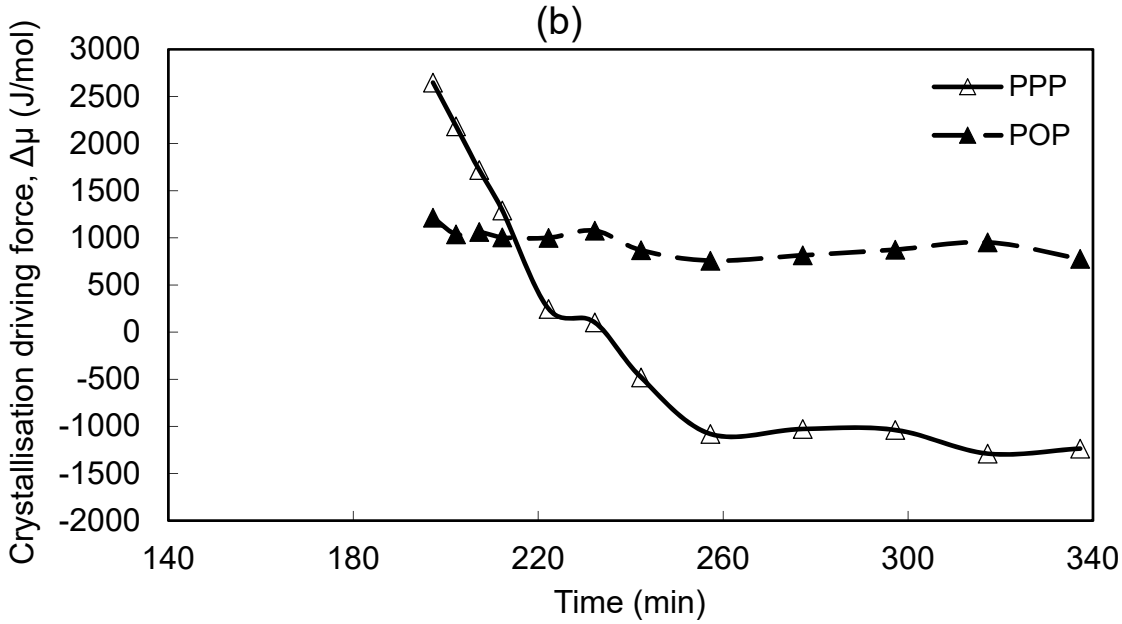
(b)
Crystallisation driving force, Δμ (J/mol)
3000
2500
2000
1500
1000
500
0
-500
-1000
-1500
-2000
140
180
220
260
300
340
Time (min)
PPP
POP

Fig. 5